Ternary Multicomponent Adsorption Modelling Using ANN, LS-SVR, and SVR Approach – Case Study

A. Yettou,[a] M. Laidi,[a,*] A. El Bey,[a] S. Hanini,[a]
M. Hentabli,[b] O. Khaldi,[c] and M. Abderrahim[a]

[a] Laboratory of Biomaterials and Transport Phenomena (LBMPT), University of Médéa, Algeria
[b] Laboratory Quality Control, Physico-Chemical Department,
Antibiotical Saidal of Médéa, Algeria
[c] Material and Environment Laboratory (LME), University Yahia Fares of Medea, Médéa, Algeria

Abstract
The aim of this work was to develop three artificial intelligence-based methods to model the ternary adsorption of heavy metal ions {Pb^{2+}, Hg^{2+}, Cd^{2+}, Cu^{2+}, Zn^{2+}, Ni^{2+}, Cr^{4+}} on different adsorbates {activated carbon, chitosan, Danish peat, Heilong-jiang peat, carbon sunflower head, and carbon sunflower stem). Results show that support vector regression (SVR) performed slightly better, more accurate, stable, and more rapid than least-square support vector regression (LS-SVR) and artificial neural networks (ANN). The SVR model is highly recommended for estimating the ternary adsorption kinetics of a multicomponent system.

Keywords
Multicomponent adsorption, heavy metals, artificial neural networks, support vector regression, least-square support vector regression

1 Introduction

Due to increasing concentrations of various toxic and non-biodegradable contaminants like heavy metals in industrial wastewater, which have an adverse effect on human health and the environment,[1] various purification techniques have been proposed for wastewater treatment; adsorption is commonly being employed because of its high removal capacity of heavy metal ions using different adsorbents, low-cost of installation, operation and maintenance, and simple design.[2] Heretofore, numerous studies have reported the simultaneous interactions of multicomponent adsorption phenomenon of heavy metal ions on the adsorbent.[3–5] To design the adsorption equipment, it is mandatory to know the adsorption mechanisms. Thus, various empirical and theoretical models have been proposed in the literature to evaluate the equilibrium adsorption of heavy metals, namely Langmuir, Freundlich, Toth, and other models.[6] Since the multicomponent adsorption process is highly complex phenomena explained by the competition and interaction nature (synergism, synergism and non-interaction)[7] between adsorbent and multiple adsorbates, as well as operating conditions (pH, time, temperature, and concentration), it is difficult to model using the theoretical models.[8]

Various artificial intelligence methods are presented in the literature to overcome the limitations of the theoretical models. Most of them are established to model the removal of a single heavy metal, but few discuss the application of these models to model the multicomponent heavy met-

al adsorption process. [9,10] ANNs are applied successfully to model the non-linear behaviour between dependent and independent variables without knowing any previous details about the physical process in complex systems.[7,11–14] However, to the best of our knowledge, very few studies are devoted to the application of LS-SVM or SVM approach to model the competitive adsorption of heavy metals.[15,16]

Therefore, the major motivation behind this study was to assess the predictability power of three modelling approaches {ANN, SVM, and LS-SVM} in modelling the nonlinear relationships between the removal capacity from aqueous solution of five ternary heavy metal systems on different adsorbents and the independent parameters. The experimental data set employed in this work to optimise the three model parameters was extracted from previously published literature. The performance of these models will be evaluated using well-known statistical metrics and compared with the experimental data.

2 Modelling approaches

2.1 ANN model

Artificial neural network (ANN) by its similarity with human brain functionality, can learn the complex relationship between the response and its effecting parameters from previous experimental data set, and can use the obtained knowledge in future predictions. The performance of the ANN depends on some parameters, such as the number of hidden layers and the number of neurons in each hidden layer, the transfer function, and the normalisation func-

* Corresponding author: Dr Maamar Laidi
Email: maamarw@yahoo.fr

tion.[17,18] The output of each hidden neuron (j) can be written in the following form in terms of inputs X_i, weights and biases, and the transfer function $f(x)$:[19]

$$H_j^O = f(\sum_{i=1}^{I} X_i \cdot W_{ij} + b_j) \tag{1}$$

The final output (k) can also be expressed in the following form:[19]

$$O_k^O = f(\sum_{j=1}^{J} H_j^O \cdot W_{jk} + b_k)$$

The transfer function, weights and biases can be determined during the training stage.

2.2 LS-SVM and SVM model

Support vector machine (SVM) presents a number of superiorities in comparison to ANN, it can map the nonlinear relationship between inputs and output(s) avoiding to be stocked into local minima, it can solve problems using only support vector and it can deal with small data set.[20,21] The performance of SVM model can be determined based on the selected kernel function and its parameters.[16] The predicted output can be expressed *via* SVM model as follows:[16]

$$y(x)_{pre} = \sum_{i=1}^{n} \alpha_i \cdot K(x_i, x_j) + b \tag{2}$$

where $K(x_i, x_j)$ can be linear, polynomial, Gaussian or radial basis function kernel. α_i and b denote Lagrange multiplier and threshold parameter, respectively. In support vector regression, it is mandatory to optimise the following expression:[16]

$$\frac{1}{2}W^2 + C\sum_{i=1}^{n} {}_{i} \tag{3}$$

where W denotes the margin and represents the complexity of the SVM model, $\sum_{i=1}^{n} {}_{i}$ represents the sum of the training errors, and C is a tuning parameter. Compared to the conventional SVM, LS-SVM can convert the inequality constraints into equality constraints.[21]

3 ANN, LS-SVR, and SVR modelling

3.1 Data set collection and processing

The data set used in this work has been collected from previously published papers in literature and organised in a matrix of {84 points, 11 parameters} including 8 inputs and 3 outputs. Table 1 presents details and sources of the selected data set.

Table 1 – Details of the used data set

Sys.	Adsorbates	Adsorbent	Data points	Ref.
1	$Pb^{2+} + Hg^{2+} + Cd^{2+}$	Activated carbon	15	22
2	$Pb^{2+} + Cu^{2+} + Zn^{2+}$	Chitosan	20	23
3	$Pb^{2+} + Cu^{2+} + Cd^{2+}$	Danish peat	10	24
		Heilongjiang peat	10	
4	$Ni^{2+} + Cr^{4+} + Cd^{2+}$	Carbon sunflower head	8	25
		Carbon sunflower stem	8	
5	$Zn^{2+} + Cu^{2+} + Cd^{2+}$	Activated carbon	13	26

The data set was divided into 8 inputs explained as follows: BET surface, structure index of each adsorbent (micropores, mesopores, macropores), molecular weight of each compound (M_{w1}, M_{w2} and M_{w3}), initial concentration for each compound (c_{e1}, c_{e2}, c_{e3}) and the removal capacity of each heavy metal ion (q_{e1}, q_{e2}, and q_{e3}) as outputs.

The data set was divided randomly: 74 % for training and 26 % for the test stage (case of SVR and LS-SVR model), and 76 % for training, 12 % for the test, and 12 % for validation (case of ANN model). In order to ensure the rapid convergence of the models, a normalisation stage of inputs was done using the proposed function expressed by expression 4, while the outputs were normalised/post-normalised using the two functions programmed in MATLAB {premnmx(Y)/postmnmx(Y)} as represented in expressions 5 and 6, respectively. The aim of the normalisation was to have the data in the same range and avoid greater errors.[21]

$$X_n = \sqrt[0.59]{x} \tag{4}$$

$$y_n = \frac{2\{Y - \min(Y)\}}{\{\max(Y) - \min(Y)\}} - 1 \tag{5}$$

$$Y = 0.5 (y_n + 1)\{\max(Y) - \min(Y)\} + \min(Y) \tag{6}$$

3.2 Performance analysis of developed models

The performance of these models was assessed using two metrics, namely, the mean squared error (MSE) and the determination coefficient (R^2):

$$MSE = \frac{1}{N}\sum_{i=1}^{N}\left(y_{i\exp} - y_{i\text{cal}}\right)^2 \tag{7}$$

$$R^2 = 1 - \frac{\sum_{i=1}^{N}(y_{i\exp} - y_{i\text{cal}})^2}{\sum_{i=1}^{N}(y_{i\exp} - \overline{Y}_{i\exp})^2} \tag{8}$$

where N is the number of points, $y_{i\exp}$, $y_{i\text{cal}}$, and $\overline{y}_{i\exp}$ are the experimental, calculated, and mean of the experimental

target vectors. These metrics explain how well the model can predict the experimental data.[27] Better accuracy of the model can be found when R^2 is close to 1 and MSE is close to 0.

4 Modelling results and discussion

4.1 ANN model

In this work, a multi-layer perceptron (MLP) was selected and trained with Levenberg-Marquardt algorithm. Hyperbolic tangent and linear function was adopted in the hidden and the output layers, respectively. Table 2 presents the mathematical expression of these two transfer functions. The flowchart of ANN model development is presented in Fig. 1. This procedure was programmed in MATLAB software.

Since there are no rules for the exact determination of the ANN parameters, a trail-and-error method was adopted and based on the obtained values of the selected metrics. Details of the best ANN model parameters are presented in Table 3.

Fig. 2 shows a comparison between the experimental and predicted values of the removal capacity of the three heavy
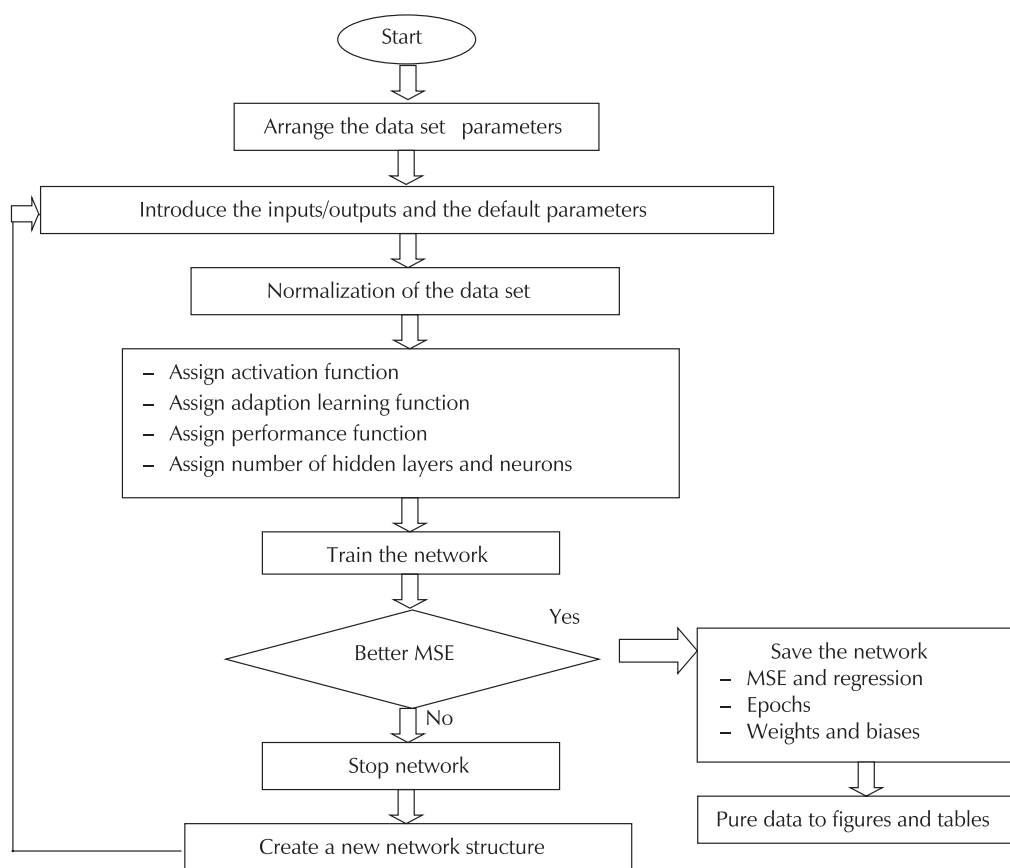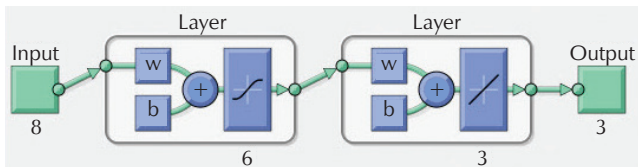

Fig. 1   – Flowchart of the ANN network development procedures

Table 2   – Expression of the transfer functions and their codes in MATLAB

Transfer function	Expression	Plot	MATLAB code
Hyperbolic tangent	$a = \dfrac{e^{+n} - e^{-n}}{e^{+n} + e^{-n}}$		*tansig*
Linear	$a = n$		*purelin*

Table 3 – Structure and parameters of the best ANN model

ANN type	Feedforward-backpropagation neural network (MATLAB code: *newff*)		
ANN structure			
Layers	Neurons number		Transfer function
Input	8		–
Hidden	6		f_h: hyperbolic tangent functions
Output	3		f_o: Linear function
Training algorithm	Levenberg-Marquardt (MATLAB code: *trainlm*)		
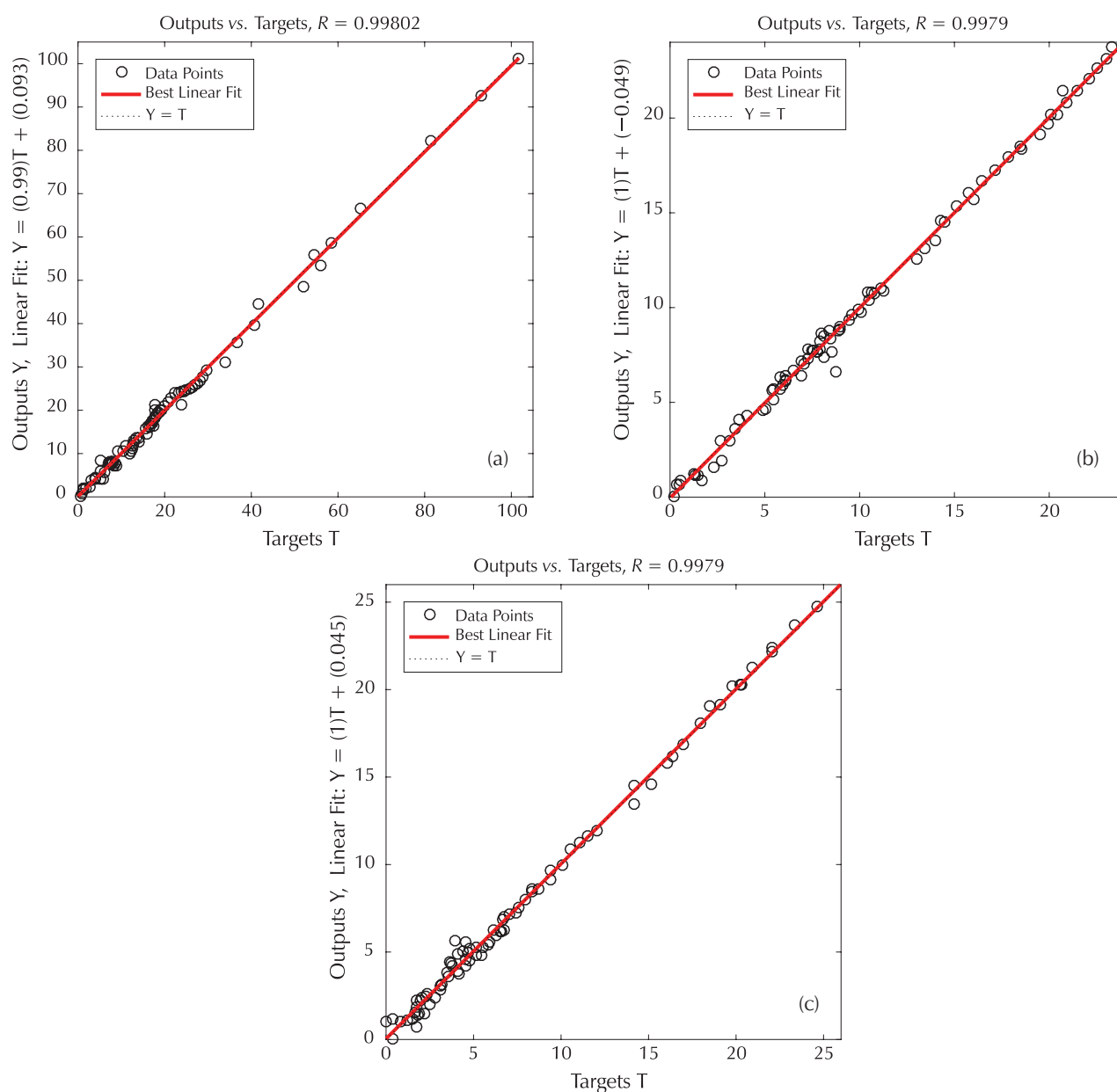
Fig. 2 – Experimental *vs.* predicted removal capacity during the generalisation stage a) for q_{e1}, b) for q_{e2}, and c) for q_{e3}

metal ions for the global data set. According to these figures, we can observe the perfect alignment of all points on the best linear fit, where the values of R^2 for the three removal capacities are superior to 0.99 during the generalisation stage. These results confirm the high ability of the obtained ANN model to capture the experimental features quite accurately.

Table 4 – Metrics comparison for the best ANN model

Statistical parameters / Removal capacity	q_{e1}	q_{e2}	q_{e3}
	Generalisation stage		
determination coefficient (R^2)	0.9960	0.9957	0.9958
correlation coefficient (R)	0.9980	0.9979	0.9979
slope (α)	0.9944	1.0038	0.9995
intercept (β)	0.0932	−0.0489	0.0454
mean squared error (MSE)	**1.4898**	**0.1780**	**0.1912**

Table 4 presents different metric comparison for the generalisation stage. It can be seen that the ANN performs well when predicting q_{e2} and q_{e3} rather than q_{e1}. Overall, the developed ANN model was found with very low MSE value and high R^2 value.

The mathematical formula that connects the inputs to each output *via* the optimised neural network (ANN) is given by equations 9 to 11:

$$q_{e1} = f_o \left(\sum_{k=1}^{6} \left(w_{1k} \cdot f_h \left(\sum_{j=1}^{8} \left(w_{kj} \cdot X_j + b_{hj} \right) \right) + b_{1k} \right) \right) \quad (9)$$

$$q_{e2} = f_o \left(\sum_{k=1}^{6} \left(w_{2k} \cdot f_h \left(\sum_{j=1}^{8} \left(w_{kj} \cdot X_j + b_{hj} \right) \right) + b_{2k} \right) \right) \quad (10)$$

$$q_{e3} = f_o \left(\sum_{k=1}^{6} \left(w_{3k} \cdot f_h \left(\sum_{j=1}^{8} \left(w_{kj} \cdot X_j + b_{hj} \right) \right) + b_{3k} \right) \right) \quad (11)$$

where w_{kj} and b_{hj} denote weights and biases between inputs-hidden layer. w_{1k} and b_{1k} denote weights and biases between hidden-output layer. f_o and f_h are linear and tangent hyperbolic transfer function. Weight and biases matrix of the proposed optimal ANN-MLP model are presented in Tables 5 and 6 to allow other researchers to reproduce results and make appropriate use of this ANN-MLP model.

An example of the comparison between experimental and predicted values is given in Fig. 3. It shows that the points
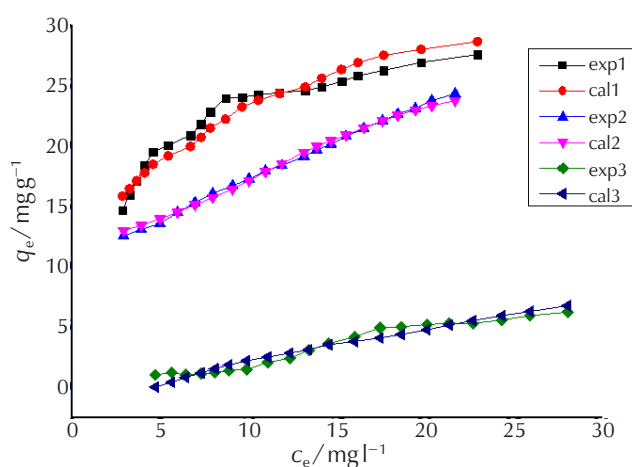

Fig. 3 – Predicted by ANN *vs* experimental removal capacity of the ternary system against concentration

Table 5 – Weights and biases values of the best ANN-MLP between inputs and hidden layer

Weight between inputs-hidden layer								bias
3.778	0.345	0.580	−3.259	3.651	−0.443	0.372	1.034	−3.018
6.121	−0.022	4.511	−4.826	1.029	−19.930	24.120	−2.290	−1.745
−702.409	4.536	−35.716	543.451	−10.606	134.855	−46.405	41.627	−48.875
58.313	−59.610	−7.310	34.432	−31.834	−0.299	0.558	0.176	56.870
159.742	−0.877	8.441	−124.056	24.288	−1.715	4.917	−5.145	15.556
−0.440	0.288	1.919	−12.676	−5.900	0.393	−0.526	−0.255	−4.160

Table 6 – Weights and biases values of the best ANN-MLP between hidden and output layer

Weight between hidden-output layer						bias
1.3632	0.0382	0.5056	21.9631	−0.7906	22.1628	−0.904
1.0129	0.2439	0.9787	54.8302	−0.1795	54.9675	−0.8653
−0.0414	−0.0639	2.1612	73.8696	2.1714	73.9097	−0.5996

predicted by ANN follow exactly and match well the trend of the experimental points, which confirms the capability of the ANN model to model the non-linear behaviour of the multicomponent adsorption system of the selected heavy metal ions.

4.2 LS-SVR model

For LS-SVR and SVR, different kernel functions have been tested to model multicomponent adsorption system. Table 7 represents the expression of these functions.

Table 7 – Kernel functions tested for LS-SVR and SVR[28]

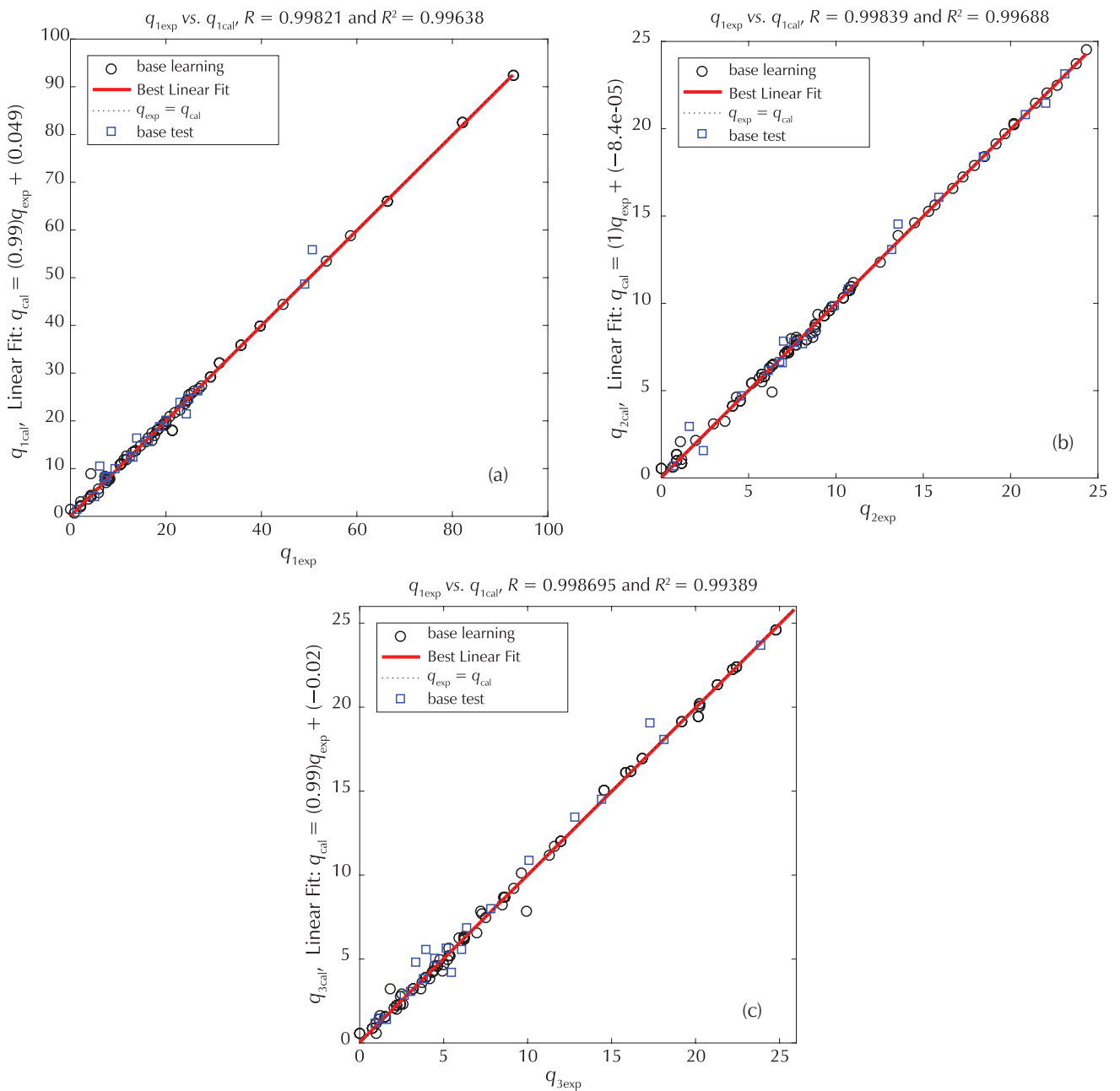| Name of the kernel	Mathematical formula
Linear kernel	$k(x,y) = x \cdot y + c$
Gaussian kernel	$k(x,y) = \exp(\dfrac{-\|x-y\|^2}{2\sigma^2})$
Radial basis function kernel	$f(x) = \sum_i^N a_i y_i \exp\left(\dfrac{-\|x-x_i\|^2}{2\sigma^2}\right) + b$
Polynomial kernel	$k(x,y) = (ax \cdot y + c)^d$

Fig. 4 – Predicted *vs* experimental adsorption capacity using LS-SVR, a) for q_{e1}, b) for q_{e2}, and c) for q_{e3}

With the selected LS-SVR structure, the maximum MSE of 1.3571 and R^2 above 0.99 were obtained during the generalisation stage. As may be seen in Fig. 4, all predicted points are very close and around the unity line, showing the satisfactory and robust LS-SVR.

The performance of the developed LS-SVR model was further analysed through the calculation of some metrics (Table 8).

4.3 SVR model

Compared to the LS-SVR and ANN models, the prediction accuracy of the SVR model was higher. Fig. 5 shows

Table 8 – Computed errors comparison results obtained by LS-SVR

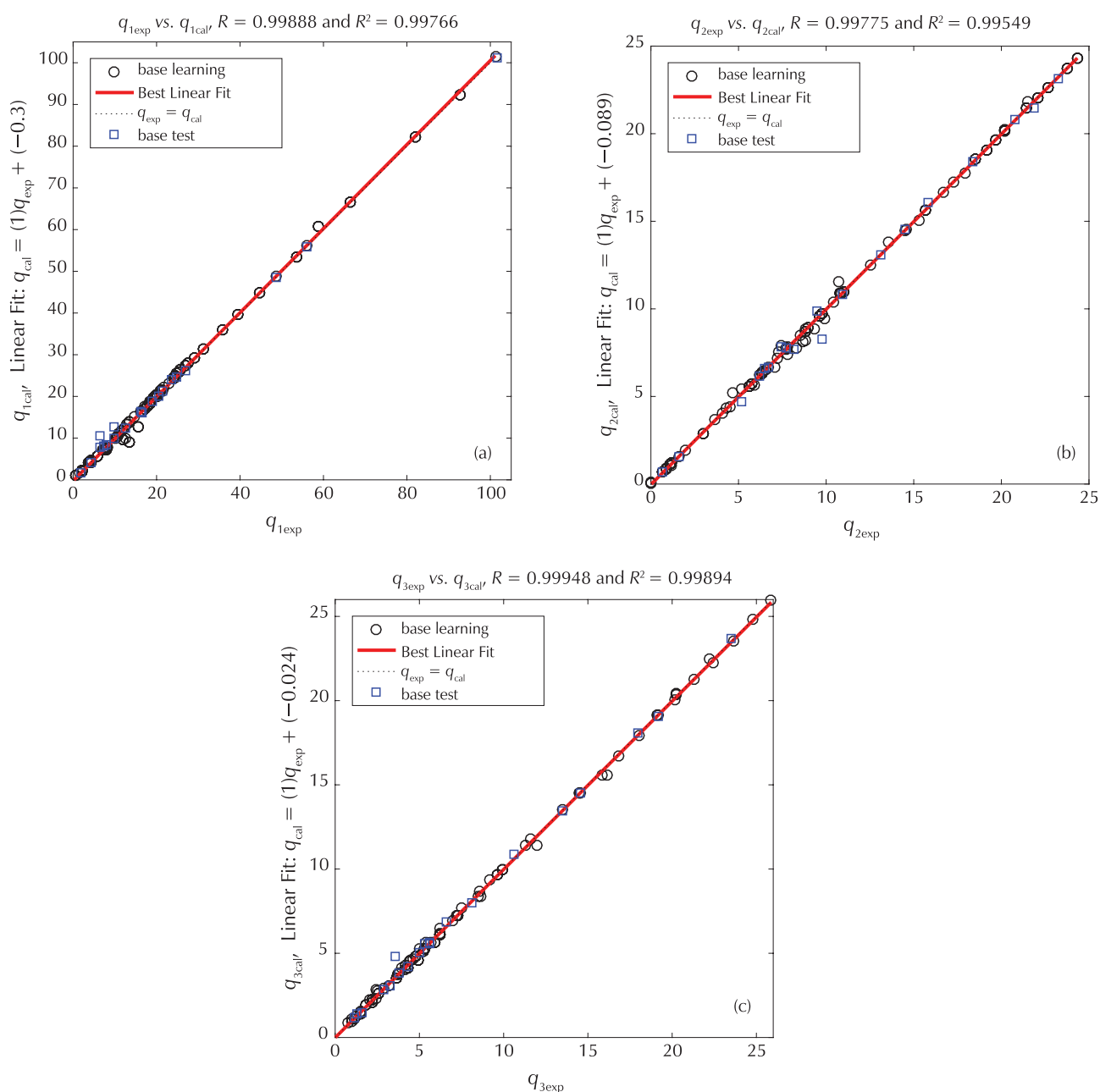| Statistical parameters \ Removal capacity	q_{e1}	q_{e2}	q_{e3}
	Generalisation stage		
determination coefficient (R^2)	0.9964	0.9969	0.9939
correlation coefficient (R)	0.9982	0.9984	0.9969
slope (α)	0.9925	0.9987	0.9920
intercept (β)	0.0488	−0.0001	−0.020
mean squared error (MSE)	**1.3571**	**0.1364**	**0.2826**

Fig. 5 – Predicted *vs* experimental adsorption capacity using SVR, a) for q_{e1}, b) for q_{e2}, and c) for q_{e3}

that R^2 was higher than 0.99, and Table 9 shows that the maximum MSE was 0.8983. This result explains the higher capability of this model in fitting the multicomponent adsorption systems.

Table 9 – Computed errors comparison results obtained by SVR

Statistical parameters \ Removal capacity	q_{e1}	q_{e2}	q_{e3}
	Generalisation stage		
determination coefficient (R^2)	0.9977	0.9955	0.9989
correlation coefficient (R)	0.9989	0.9977	0.9995
slope (α)	1.0093	1.0055	0.9990
intercept (β)	−0.3023	−0.0893	−0.024
mean squared error (MSE)	**0.8983**	**0.1957**	**0.0482**

By comparison, ANN and LS-SVR with SVR, the latter shows good performance in prediction accuracy and computational speed (Fig. 6).
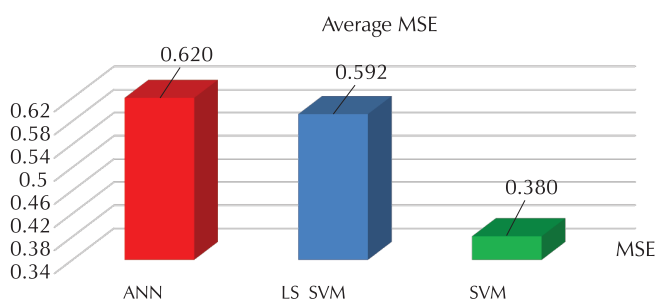

Fig. 6 – Average MSE obtained by ANN, LS-SVR, and SVR

5. Conclusions

This work aimed to model a ternary adsorption system of different heavy metals on several adsorbents, using ANN, SVR, and LS-SVR models. The optimised static neural network was found with a structure of {8-6-3}, tangent sigmoid activation function for the hidden and the linear for the output layer, Levenberg-Marquardt learning algorithm. The best ANN was found with a coefficient of determination R^2 = [0.9960, 0.9957, 0.9958] and a mean squared error MSE = [1.4898, 0.1780, 0.1912] for the three outputs for the global data set. The optimised least squared support vector regression model was found with a coefficient of determination R^2 = [0.9964, 0.9969, 0.9939] and a mean squared error (MSE) = [1.3571, 0.1364, 0.2826] for the three outputs for the global data set. The optimised support vector regression model was found with a coefficient of determination R^2 = [0.9977, 0.9955, 0.9989] and a mean squared error (MSE) = [0.8983, 0.1957, 0.0482] for the three outputs and for the global data set.

The obtained results showed that the three models exhibited good aptitudes for predicting the adsorbed quantities, although a slight preference goes for the SVR model.

References
Literatura

1. *Y. Sheth, S. Dharaskar, M. Khalid, S. Sonawane*, An environment friendly approach for heavy metal removal from industrial wastewater using chitosan based biosorbent: A review, Sustain. Energy Technol. Assess. **43** (2021) 100951, doi: https://doi.org/10.1016/j.seta.2020.100951.

2. *N. H. Yusof, K. Y. Foo, B. H. Hameed, M. H. Hussin, H. K. Lee, S. Sabar*, One-step synthesis of chitosan-polyethyleneimine with calcium chloride as effective adsorbent for Acid Red 88 removal, Int. J. Biol. Macromol. **157** (2020) 648–658, doi: https://doi.org/10.1016/j.ijbiomac.2019.11.218.

3. *B. Anna, M. Kleopas, S. Constantine, F. Anestis, B. Maria*, Adsorption of Cd(II), Cu(II), Ni(II) and Pb(II) onto natural bentonite: study in mono- and multi-metal systems, Environ. Earth Sci. **73** (2015) 5435–5444, doi: https://doi.org/10.1007/s12665-014-3798-0.

4. *C. Namasivayam, D. Sangeetha, R. Gunasekaran*, Removal of anions, heavy metals, organics and dyes from water by adsorption onto a new activated carbon from Jatropha husk, an agro-industrial solid waste, Process Saf. Environ. Prot. **85** (2007) 181–184, doi: https://doi.org/10.1205/psep05002.

5. *A. Maleki, B. Hayati, F. Najafi, F. Gharibi, S. W. Joo*, Heavy metal adsorption from industrial wastewater by PAMAM/TiO$_2$ nanohybrid: Preparation, characterization and adsorption studies, J. Mol. Liquid. **224** (2016) 95–104, doi: https://doi.org/10.1016/j.molliq.2016.09.060.

6. *M. E. Mesquita, J. M. Vieira e Silva*, Preliminary study of pH effect in the application of Langmuir and Freundlich isotherms to Cu-Zn competitive adsorption, Geoderma **106** (2002) 219–234, doi: https://doi.org/10.1016/S0016-7061(01)00125-2.

7. *P. S. Pauletto, G. L. Dotto, N. P. G. Salau*, Optimal artificial neural network design for simultaneous modeling of multicomponent adsorption, J. Mol. Liquid. **320** (2020) 114418, doi: https://doi.org/10.1016/j.molliq.2020.114418.

8. *E. Byvatov, U. Fechner, J. Sadowski, G. Schneider*, Comparison of Support Vector Machine and Artificial Neural Network Systems for Drug/Nondrug Classification, J. Chem. Inf. Comput. Sci. **43** (2003) 1882–1889, doi: https://doi.org/10.1021/ci0341161.

9. *R. M. Aghav, S. Kumar, S. N. Mukherjee*, Artificial neural network modeling in competitive adsorption of phenol and resorcinol from water environment using some carbonaceous adsorbents, J. Hazard. Mater. **188** (2011) 67–77, doi: https://doi.org/10.1016/j.jhazmat.2011.01.067.

10. *A. R. Bagheri, M. Ghaedi, A. Asfaram, S. Hajati, A. M. Ghaedi, A. Bazrafshan, M. R. Rahimi*, Modeling and optimization of simultaneous removal of ternary dyes onto copper sulfide nanoparticles loaded on activated carbon using second-derivative spectrophotometry, J. Taiwan Inst. Chem. Eng. **65** (2016) 212–224, doi: https://doi.org/10.1016/j.jtice.2016.05.004.

11. *P. S. Pauletto, J. O. Gonçalves, L. A. A. Pinto, G. L. Dotto, N. P. G. Salau*, Single and competitive dye adsorption onto chitosan–based hybrid hydrogels using artificial neural network modeling, J. Colloid Interface Sci. **560** (2020) 722–729, doi: https://doi.org/10.1016/j.jcis.2019.10.106.

12. *D. I. Mendoza-Castillo, H. E. Reynel-Ávila, F. J. Sánchez-Ruiz, R. Trejo-Valencia, J. E. Jaime-Leal, A. Bonilla-Petriciolet*, In-

sights and pitfalls of artificial neural network modeling of competitive multi-metallic adsorption data, J. Mol. Liquid. **251** (2018) 15–27, doi: https://doi.org/10.1016/j.molliq.2017.12.030.

13. *A. Gopinath, B. G. Retnam, A. Muthukkumaran, K. Aravamudan*, Swift, versatile and a rigorous kinetic model based artificial neural network surrogate for single and multicomponent batch adsorption processes, J. Mol. Liquid. **297** (2020) 111888, doi: https://doi.org/10.1016/j.molliq.2019.111888.

14. *P. S. Pauletto, S. F. Lütke, G. L. Dotto, N. P. G. Salau*, Forecasting the multicomponent adsorption of nimesulide and paracetamol through artificial neural network, Chem. Eng. J. (2020) 127527, doi: https://doi.org/10.1016/j.cej.2020.127527.

15. *J. J. González Costa, M. J. Reigosa, J. M. Matías, E. F. Covelo*, Soil Cd, Cr, Cu, Ni, Pb and Zn sorption and retention models using SVM: Variable selection and competitive model, Sci. Total Environ. **593–594** (2017) 508–522, doi: https://doi.org/10.1016/j.scitotenv.2017.03.195.

16. *Y. Wang, J. Chen, W. Tang, D. Xia, Y. Liang, X. Li*, Modeling adsorption of organic pollutants onto single-walled carbon nanotubes with theoretical molecular descriptors using MLR and SVM algorithms, Chemosphere **214** (2019) 79–84, doi: https://doi.org/10.1016/j.chemosphere.2018.09.074.

17. *Z. U. Ahmad, L. Yao, Q. Lian, F. Islam, M. E. Zappi, D. D. Gang*, The use of artificial neural network (ANN) for modeling adsorption of sunset yellow onto neodymium modified ordered mesoporous carbon, Chemosphere **256** (2020) 127081, doi: https://doi.org/10.1016/j.chemosphere.2020.127081.

18. *M. Moussaoui, M. Laidi, S. Hanini, M. Hentabli*, Artificial Neural Network and Support Vector Regression Applied in Quantitative Structure-property Relationship Modelling of Solubility of Solid Solutes in Supercritical CO_2, Kem. Ind. **69** (11-12) (2020) 611–630, doi: https://doi.org/10.15255/KUI.2020.004.

19. *Y. Kumar, L. Singh, V. S. Sharanagat*, A. Tarafdar, Artificial neural network (ANNs) and mathematical modelling of hydration of green chickpea, Inf. Process. Agricult. (2020) 1–12, doi: https://doi.org/10.1016/j.inpa.2020.04.001.

20. *L.-J. Cao, F. E. H. Tay*, Support vector machine with adaptive parameters in financial time series forecasting, IEEE Trans. Neural Netw. **14** (2003) 1506–1518, doi: https://doi.org/10.1109/tnn.2003.820556.

21. *S. Zhou, X. Chu, S. Cao, X. Liu, Y. Zhou*, Prediction of the ground temperature with ANN, LS-SVM and fuzzy LS-SVM for GSHP application, Geothermics **84** (2020) 101757, doi: https://doi.org/10.1016/j.geothermics.2019.101757.

22. *K. Kadirvelu, J. Goel, Cjj. Rajagopal*, Sorption of lead, mercury and cadmium ions in multi-component system using carbon aerogel as adsorbent, J. Hazard. Mater. **153** (2008) 502–507, doi: https://doi.org/10.1016/j.jhazmat.2007.08.082.

23. *Y. Zhu, J. Hu, J. Wang*, Competitive adsorption of Pb (II), Cu (II) and Zn (II) onto xanthate-modified magnetic chitosan, J. Hazard. Mater. **221** (2012) 155–161, doi: https://doi.org/10.1016/j.jhazmat.2012.04.026.

24. *F. Qin, B. Wen, X.-Q. Shan, Y.-N. Xie, T. Liu, S.-Z. Zhang, S. U. Khan*, Mechanisms of competitive adsorption of Pb, Cu, and Cd on peat, Environ. Pollut. **144** (2006) 669–680, doi: https://doi.org/10.1016/j.envpol.2005.12.036.

25. *M. Jain, V. K. Garg, K. Kadirvelu, M. Sillanpää*, Adsorption of heavy metals from multi-metal aqueous solution by sunflower plant biomass-based carbons, Int. J. Environ. Sci. Technol. **13** (2016) 493–500, doi: https://doi.org/10.1007/s13762-015-0855-5.

26. *D. Mohan, K. P. Singh*, Single-and multi-component adsorption of cadmium and zinc using activated carbon derived from bagasse – an agricultural waste, Water Res. **36** (2002) 2304–2318, doi: https://doi.org/10.1016/S0043-1354(01)00447-X.

27. *C. M. Amado, C. J. Minahk, E. Cilli, G. Oliveira, F. G. Dupuy*, Bacteriocin enterocin CRL35 is a modular peptide that induces non-bilayer states in bacterial model membranes, BBA – Biomembranes **1862** (2) (2019) 183135, doi: https://doi.org/10.1016/j.bbamem.2019.183135.

28. *H. Benimam, C. Si-Moussa, M. Laidi, S. Hanini*, Modeling the activity coefficient at infinite dilution of water in ionic liquids using artificial neural networks and support vector machines, Neural Comput. Appl. **32** (2020) 8635–8653, doi: https://doi.org/10.1007/s00521-019-04356-w.

SAŽETAK

Ternarno višekomponentno modeliranje adsorpcije primjenom ANN-a, LS-SVR-a i SVR-a – studija slučaja

Amina Yettou,[a] *Maamar Laidi,*[a,*] *Abdelmadjid El Bey,*[a] *Salah Hanini,*[a] *Mohamed Hentabli,*[b] *Omar Khaldi,*[c] and *Mihoub Abderrahim*[a]

Cilj ovog rada bio je razviti tri metode temeljene na umjetnoj inteligenciji za modeliranje trostruke adsorpcije iona teških metala {Pb^{2+}, Hg^{2+}, Cd^{2+}, Cu^{2+}, Zn^{2+}, Ni^{2+}, Cr^{4+}} na različitim adsorbatima {aktivni ugljen, kitozan, danski treset, treset Heilongjiang, ugljik glave suncokreta i ugljik stabljike suncokreta). Rezultati pokazuju da se regresija potpornih vektora (SVR) pokazala nešto boljom, preciznijom, stabilnijom i bržom od regresije potpornih vektora najmanjih kvadrata (LS-SVR) i umjetnih neuronskih mreža (ANN). Za procjenu kinetike trostrukog adsorpcijskog sustava višekomponentnog sustava preporučuje se model SVR.

[a] *Laboratory of Biomaterials and Transport Phenomena (LBMPT),*
 University of Médéa, Algeria
[b] *Laboratory Quality Control,*
 Physico-Chemical Department,
 Antibiotical Saidal of Médéa, Algeria
[c] *Material and Environment Laboratory (LME),*
 University Yahia Fares of Medea,
 Médéa, Algeria